Study of the Bond Behavior of Concrete Beam Strengthened with NSM-CFRP

N. Chikh, A. Merdas, A. Laraba, R. Benzaid

Abstract—**The Near Surface Mounted (NSM) technique has been used in recent years for the strengthening of reinforced concrete beams. It involves the insertion of strips or rods of carbon fibers reinforced polymers (CFRP) in grooves made previously in the concrete cover of corresponding surfaces, filled with epoxy adhesive for fixation. In order to characterize the laminate and rods to concrete bond behavior, an experimental work based on pullout-bending tests was carried out. The pullout load on the composite and the slip at the free and loaded ends were measured. The influences of the concrete strength, the type and the configuration of the reinforcement, and the embedded length on the bond behavior between the three materials (concrete, epoxy adhesive and CFRP) were evidenced and compared.**

Index Terms— **Beam, NSM-CFRP, bond, pullout-bending**

I. INTRODUCTION

Structural repair and strengthening of concrete structures are becoming increasingly important options for deteriorated structures. The use of composites materials is a remarkable strengthening technique for increasing and upgrading the flexural load carrying capacity of reinforced concrete members. One of the popular methods in the strengthening of RC beams is by providing externally bonded reinforcement (EBR) made of fiber reinforced polymer (FRP) laminates for additional flexural resistance. However, many tests carried out on RC beams strengthened for flexure with externally bonded FRP materials indicated low efficiency of this technique, caused by premature FRP debonding failure. Furthermore, EBR technique is susceptible to damage from collision, fire, temperature variation and ultraviolet rays. Near surface mounted (NSM) technique has become promising and attractive for flexural strengthening of RC beams. The NSM technique consists in applying carbon fiber-reinforced polymer (CFRP) laminate strips into slits opened in the concrete cover of the elements to be strengthened. A normal cold cured epoxy based adhesive is used to bond the CFRP laminate strips to concrete (Fig. 1). Due to better anchorage of embedded NSM FRP reinforcement, this technique has been significantly more efficient than EBR system. Several experimental tests indicated benefits of NSM technique such
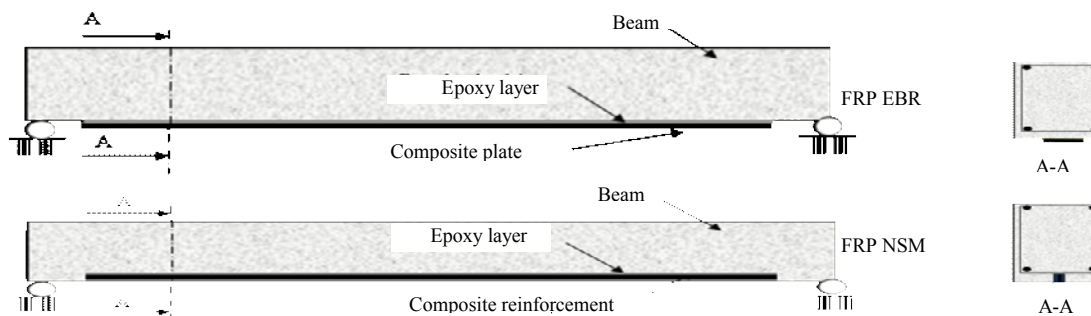
Fig.1. Principle of EBR and NSM strengthening

N. Chikh is with the Civil Engineering Department, Laboratory of Materials and Durabilité of Constructions (L.M.D.C), University of Constantine 1, Constantine 25000, Algeria.(phone: 213-77370-3026; fax: 213-3181-8967; e-mail: chikh_ne@yahoo.fr).

A. Merdas is with the Civil Engineering Department, University of Sétif, 19000, Algeria.(phone: 213-66213-3148; fax: 213-3181-8967; e-mail: abdelghani.merdas@yahoo.com).

A. Laraba is with the Civil Engineering Department, Laboratory of Materials and Durabilité of Constructions (L.M.D.C), University of Constantine 1, Constantine 25000, Algeria.(phone: 213-55635-6916; e-mail: abdelkrim.laraba@hotmail.fr).

R. Benzaid is with the Civil Engineering Department, Laboratory of Geology Engineering (L.G.G), University of Jijel, Jijel 18000, Algeria. (phone: 213-55048-2482; e-mail: Benzaid_riad@yahoo.fr).

as: increase in the load carrying capacity of RC members, easy to apply and cost effective [1] and [2]. However, the performance of the NSM technique seems to be controlled entirely by the bond behavior of the interface laminate-adhesive-concrete, [3], [4], [5] and [6].

For this purpose, an experimental investigation has been carried out through pullout-bending tests. The influence of the following parameters has been considered:

--Type of concrete: two ordinary concretes (C30, C50) and one high performance concrete (HPC75).

--Bond length Lb: 120mm, 80mm and 40 mm.

--Type of reinforcement: smooth carbon rod (SCR) and smooth carbon plate (SCP).

Two configurations (Fig.2) were considered for the last reinforcing technique:

-- A plate fully inserted in the groove (SCPF).

-- A plate partially inserted in the groove (SCPP). This situation simulates the case of insufficient concrete cover depth or the case where the cutting of the bottom transverse steel is to be avoided. Obviously, a new layer of repairing concrete will be bonded to the existing concrete.
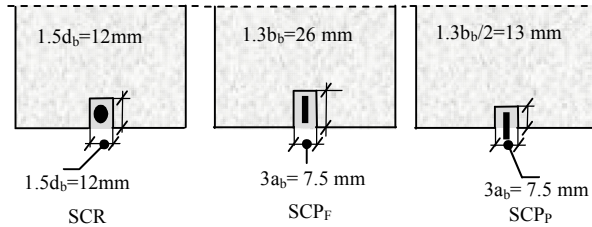
Fig.2. CFRP reinforcement configurations

Tests with deformed steel bars (DSB) were also performed for comparison purpose.

I. STUDY OF MATERIAL PROPERTIES

A. Carbon reinforcements (plate and rod)

CFRP plates and rods are provided by the company SOFICAR France ®. They are composed of unidirectional carbon fiber embedded in epoxy adhesive matrix. They have similar cross section of 50 mm². Their main properties according to the manufacturer are as follows: 160 GPa for elastic modulus, 3000 MPa for tensile strength and 2.0% for elongation at break. To evaluate the tensile strength and the Young's modulus, uniaxial tensile tests were conducted with 200 kN maximum capacity hydraulic tensile machine.

The test was performed in a load-control mode with a constant rate of 0.1kN/s, until the failure of the reinforcement.

Stress–strain curve of CFRP plates and rods is linear up to the point of failure without any yielding. The following values of 2500 MPa, 160 GPa and 1.50%, represent respectively, the tensile strength, the Young's modulus and the ultimate strain at break of the composite.

B. Epoxy resin

EPONAL 371 was the type of resin used for filling grooves. It is manufactured by the company BOSTIK France®. Its properties according to the manufacturer are given in the following table:

TABLE I
EPONAL 371 PROPERTIES

Type of epoxy adhesive	EPONAL 371
Tensile strength (MPa)	31.7 ±3.2
Elongation at break (%)	1.2 ± 0.3
Young's modulus (MPa)	3800 ±130
Compressive strength (MPa)	76.8 ± 0.8
Compression (%)	4.2 ± 0.2
Young's modulus (MPa)	3400 ± 250

Characterization tests were carried out using the Instron testing machine (series 5565) equipped with an extensometer (± 5mm) to measure the deformation of the specimens, in displacement control mode with a constant rate of 0.01mm/mn. Small effect of curing time between 7 and 10 days was observed, the tensile strength at 10 days was slightly higher than that at 7 days. From ten tests, an average tensile strength of 29 MPa was obtained with a standard deviation (SD) of 4.28 MPa and a coefficient of variation (CV) of 0.15%.

Compression tests were conducted in accordance with ASTM D 695 M-91 standard. Testing was conducted on two sets of specimens, one after 7 and another one after 10 days of curing. The tests were conducted on a 250-kN universal testing machine in displacement control mode, with a cross-head displacement rate of 1.0 mm/min. From ten tests, an average compressive strength of 60.86 MPa was obtained with a standard deviation (SD) of 3.10 MPa and a coefficient of variation (CV) of 5.44%.

C. Concretes

Three types of vibrated concretes were studied: two ordinary concretes (C30) and (C50) and one high performance concrete (HPC75). The ordinary concrete C30 and C50 were made with cement, water, sand and aggregates and mixed proportion defined in Table 2. In addition to these constituents, a superplasticizer was added to the mixture for the manufacture of high performance concrete HPC75. Aggregates used in the skeleton of the three concrete are fine sand (0-4 mm), and gravel (6-20 mm).

After casting, the specimens were stored for 28 days in plastic containers filled with water (20° C). The properties of hardened concrete, compressive strength fcm and elastic modulus Ec, were obtained by compression test performed on 16cm x 32cm specimens, according to the French NF P 18-406 standard. Tensile strength fctm was obtained by splitting tests in accordance with NF P 18-406 standard. All the results are gathered in Table II.

TABLE II
MECHANICAL PROPERTIES OF CONCRETES

Constituents	C30	C50	HPC75
Total water (l/m³)	209	170	150
Cement CEM I 52.5 (kg/m³)	336	400	500
Sand 0 / 4 (kg/m³)	419	451	715
Fine gravel (4/10) (kg/m³)	471	507	/
Gravel 6.3/20 (kg/m³)	834	897.5	987
Superplasticizer (kg/m³)	/	/	4.71
W/C	0.62	0.42	0.3
G/C	2.48	2.24	1.97
Compressive strength fcm (MPa)	37.5	57	73.5
Tensile strength fctm (MPa)	2.97	4.73	6.01
Modulus of elasticity E_c (GPa)	33.55	40,56	47.88

II. EXPERIMENTAL METHODOLOGY

The specimens were prepared at the age of 28 days. The two blocks composing each specimen were removed from the curing room to make the grooves using a table-mounted circular saw. In order to eliminate the dust from the sawing process, the grooves were cleaned with water under pressure. To ensure a dry surface before bonding the laminate to the concrete, the specimens were air-dried in the

laboratory environment during two weeks. Prior to CFRP installation, the width and the depth of the groove size, in the test region, were measured.

Before bonding the CFRP, the grooves were again cleaned by compressed air (Fig. 3). To avoid epoxy adhesive in undesirable zones, a masking procedure was adopted. The CFRP was cleaned using acetone.

Fig.3. Strengthening of test specimens

A.   Configuration of the test system

The test layout adopted is similar to that proposed by RILEM [7] to evaluate the bond characteristics of conventional steel rebars. The dimensions of the concrete specimen were modified to use the available moulds. Figure 4 shows the pullout-bending test adopted in this work. A beam test, consisting of two rectangular concrete blocks (A and B), connected through a steel hinge in the top part, and by the CFRP laminate or rod at the bottom, is stressed in simple bending (4 points) by two equal forces and arranged symmetrically about the midsection of the beam. Subjecting the beam to a vertical load will cause traction in rod or plate.

In addition, during loading, the point of the resultant of the internal forces is known. The compressive force in the beam at midspan is located in the center of the steel hinge while the lever arm of the internal moment is constant for any level of load. This allows an accurate calculation of
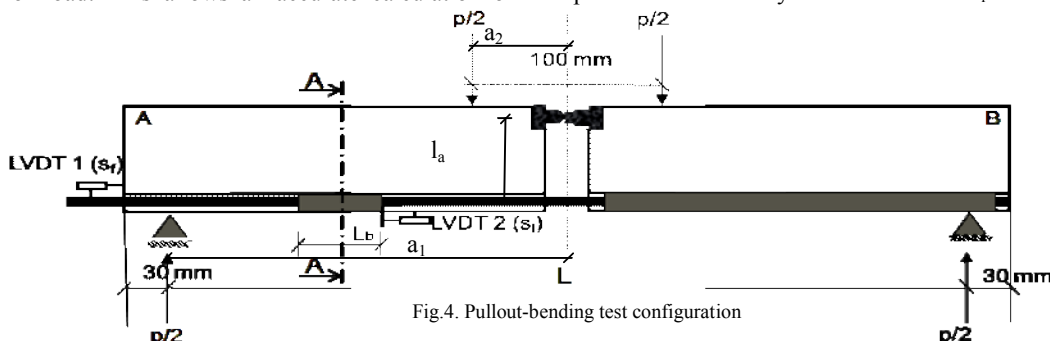
tensile strength and stresses induced in the carbon rod and plate.

The bond test region was localized in block A, using distinct bond lengths, L_b. To ensure negligible slip of the plate or rod fixed to block B, a bond length of 320 mm was considered. This also ensures that the bond failure occurs in block A.

The various tests were performed in the laboratory L2MGC, University of Cergy-Pontoise, using the Instron testing machine (series 5565) with a load driven on the rate (0.25mm/mn).

To measure the slip of the CFRP reinforcement, two displacement transducers (LVDT1 and LVDT2) of 10mm nominal stroke were applied (Figure 4). LVDT1 recorded the slip at the free end S_f, while LVDT2 measured the slip at the loaded end S_l. On the basis of equilibrium conditions, the force P measured with the load cell was used to evaluate the pullout force F on the CFRP, as follows:

$$F = \frac{P(a_1 - a_2)}{2l_a} \qquad (1)$$

Depending on the size and type of the reinforcement, the following relations were obtained:

$F_R = 1.86P$ (SCR)
$F_{PF} = 2.13P$ (SCP$_F$)
$F_{PP} = 1.35P$ (SCP$_P$)

III.   EXPERIMENTAL RESULTS

A.   General behaviour

Typical curves representing the pullout force versus slip at the loaded and free end are displayed in Figures 5 and 6 (for a bond length equal to 40 mm, and a C30 concrete strength).

The sequences observed are as follows: for loads less than 30% of the maximum pullout force (Fmax), no visible cracks occurred at the resin and concrete but a small slip between the bonded CFRP composite and the surrounding concrete was recorded by the LVDT2, resulting in a linear increase in bond stress. Then, as the applied load increased, a first slip was recorded at the free end of the reinforcement.

Beyond 0.4 Fmax, the slip becomes increasingly nonlinear due to the plasticization   of the epoxy resin, resulting in the separation process at the composite-resin and resin-reinforced concrete interfaces.

At the peak where the ultimate bond stress is reached, the slip increases brutally in both ends S_l and S_f of the

Fig.4. Pullout-bending test configuration

reinforcement, and the curve drops in a nonlinear manner until the end point of rupture. This transition is due to the degradation of the mechanism of bond at the composite-resin-concrete interface.
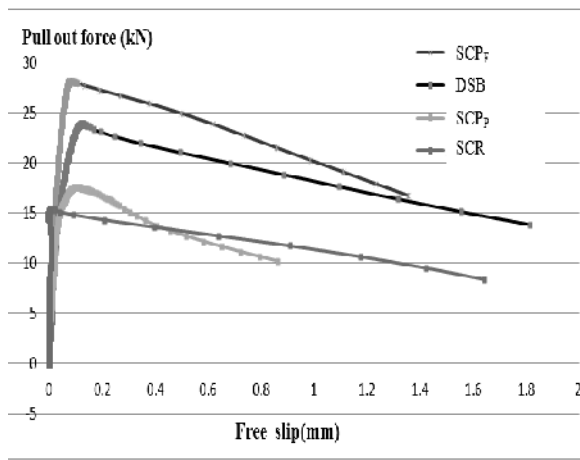
Fig.5. Typical Load-slip curves at free end
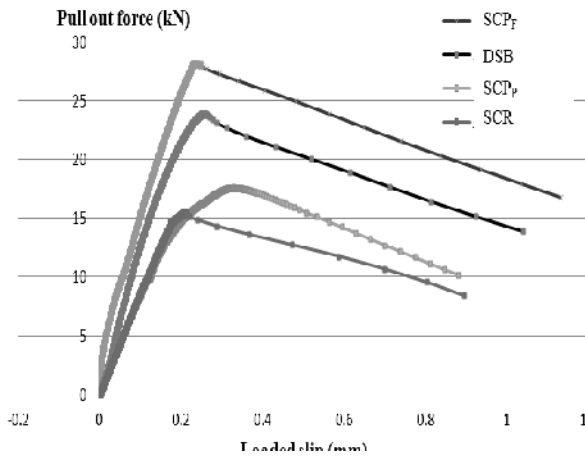
Fig.6. Typical Load-slip curves at loaded end

Fig.7. Bond failure modes

Where:

    Fmax: the maximum applied pullout force (N);

    ϕ and w_f : respectively the diameter of the rod (mm)

    and the width of the plate (mm);

    L_b : the bond length (mm).

    The results from the different test series are shown in Table III which also indicates the value of the pullout rigidity (K_l), calculated by linear regression for loads between 20% and 80% of the tensile strength.

Different failure modes were observed such as: mixed interfacial failure (composite-epoxy/epoxy-concrete) with a concrete cracking forming a diagonal splitting cracks pattern as shown in Fig.7a, rupture of concrete surrounding the groove (Fig.7b), failure with facial slip between composite and epoxy (Fig.7c). Their occurrence depends on the considered parameters and in particular the bond length.

A.   *Bond stress*

The average ultimate bond stress was calculated by the following relations:

$$\tau_u = \frac{F_{max}}{\pi \phi L_b} \quad \text{(SCR)} \tag{2}$$

$$\tau_u = \frac{F_{max}}{2 w_f L_b} \quad \text{(SCP}_F\text{)} \tag{3}$$

$$\tau_u = \frac{F_{max}}{w_f L_b} \quad \text{(SCP}_P\text{)} \tag{4}$$

TABLE III
RESULTS OF DIFFERENT SERIES

Designation	Concrete	L_b (mm)	F_{max} (kN)	τ_u (MPa)	K_l (kN/mm)
SCR	C30	40	16.55	16.47	26.20
SCR	C30	80	22.71	11.30	44.85
SCR	C30	120	33.37	11.07	68.05
SCR	C50	40	22.08	21.98	32.13
SCR	C50	80	30.57	15.21	55.11
SCR	C50	120	40.78	13.53	67.98
SCR	HPC75	40	23.01	22.90	48.28
SCR	HPC75	80	34.52	17.18	57.50
SCR	HPC75	120	46.02	15.27	74.88
DSB	C30	40	18.22	18.13	54.67
DSB	C30	80	26.60	13.24	59.39
DSB	C30	120	29.09	9.65	72.65
SCP$_F$	C30	40	21.35	13.34	44.03
SCP$_F$	C30	80	31.55	9.86	61.05
SCP$_F$	C30	120	41.70	8.69	67.47
SCP$_F$	C50	40	27.66	17.29	45.67
SCP$_F$	C50	80	36.93	11.54	64.06
SCP$_F$	C50	120	44.65	9.30	79.72
SCP$_F$	HPC75	40	29.12	18.20	60.38
SCP$_F$	HPC75	80	37.22	11.63	65.66
SCP$_F$	HPC75	120	47.62	9.92	79.11
SCP$_P$	C30	40	17.39	21.74	65.70
SCP$_P$	C30	80	30.12	18.83	80.69
SCP$_P$	C30	120	36.53	15.22	81.58

1)   *Effect of type of reinforcement*

The maximum resistance obtained by the different configurations of composite strengthening is illustrated in Figs. 8 and 9. A better performance was achieved by of carbon plates (SCP_F and SCP_P) compared to carbon rods (SCR). For similar cross section, the reinforcement SCP_F provides a greater contact surface area so that a greater pullout force is achieved. Although, the configuration SCP_P has approximately the same contact surface as the configuration SCR, a greater resistance to pull out is recorded in this case. This may be attributed to the smaller average thickness of the adhesive which best matches the reinforcement geometry and grooves.

The deformed steel bars present a rough surface allowing a better adhesion with surrounding concrete compared to SCP_F and SCR. In this case, the ribs on the surface of the bars prevent the failure of a grip and the tensile strength of the reinforcement which limits pullout force. These results show a strong effect of the micro-geometry of the reinforcements.
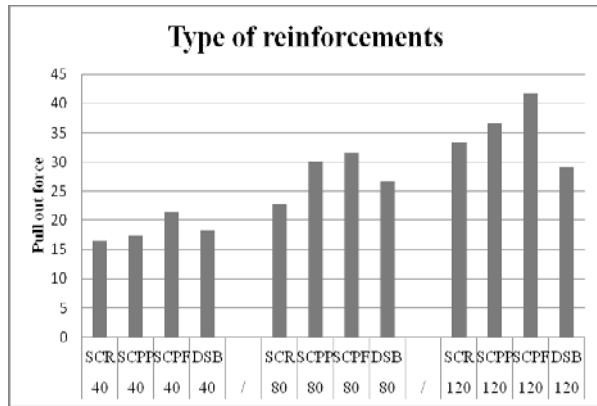
Fig.8. Effect of type of reinforcement for C30
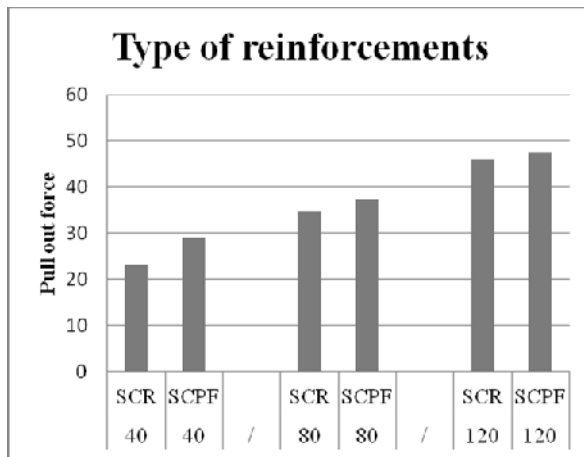
Fig.9. Effect of type of reinforcement forHPC75

2)   *Effect of bond length*

The variation of the maximum pullout force regarding the increase of the bond length L_b. is illustrated in Figs. 10 and 11. It is observed that the pullout force increases almost linearly with increasing bond length for the three types of concrete tested.
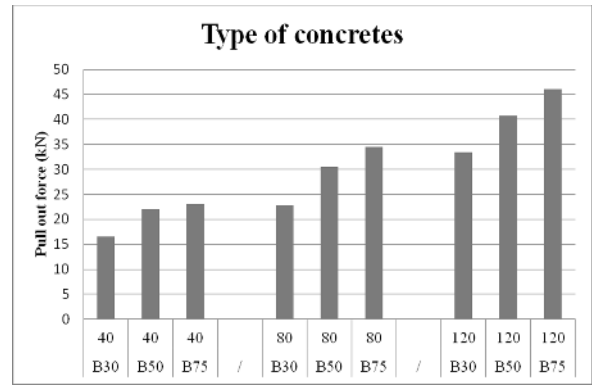
Fig.10. Effect of bond length for C30
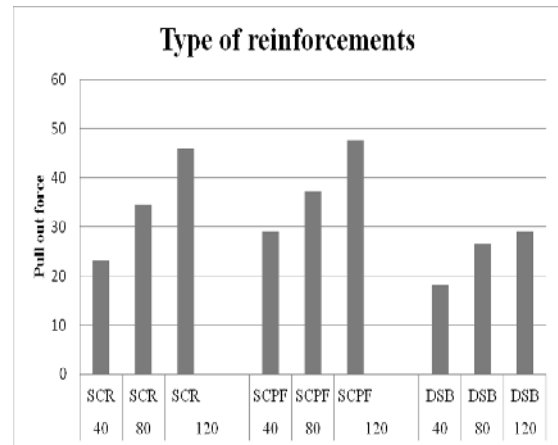
Fig.11. Effect of bond length for HPC75

3)   *Effect of concrete strength*

In all cases, the resistance to pull out improves with increasing concrete strength as indicated by Figs. 12 and 13. This influence is more pronounced for smaller bond lengths (L_b=40 mm). The optimum appears to be achieved with L_b=120 mm, where the effect of concrete strength is reduced.
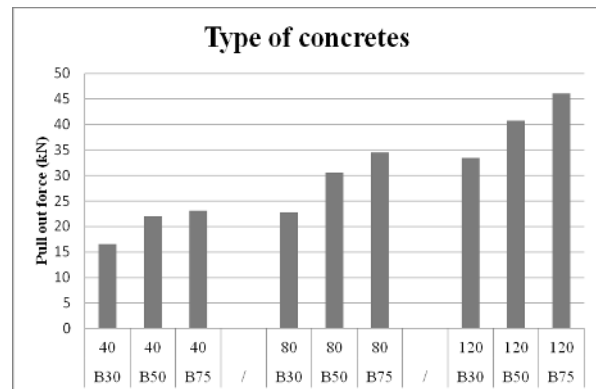
Fig.12. Effect of concrete strength for SCR
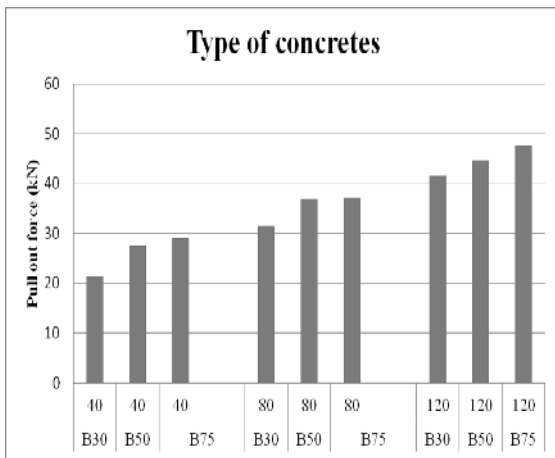
Fig.13. Effect of concrete strength for SCP$_F$

IV. CONCLUSION

Bond tests were performed by bending to characterize the bond behavior of carbon reinforcements positioned in the concrete by the NSM method. The influence of the type of reinforcement, the concrete strength and the embedded length were considered. From the results obtained, the following comments can be made:

A better performance was achieved by of carbon plates compared to carbon rods.

The pullout force increases almost linearly with the bond length for the three types of concrete tested.

The resistance to pull out improves with increasing concrete strength and this influence is more pronounced for smaller bond lengths.

ACKNOWLEDGMENT

REFERENCES

[1] J.A.O., Barros, A.S. Fortes, "Concrete beams reinforced with carbon laminates bonded into slits", in *Proceedings of 5° Congreso de Métodos Numéricos en Ingenieria*, Madrid, Spain, 2002, pp.1-6.
[2] De. Lorenzis, J.G. Teng, "Near-surface mounted FRP reinforcement: An emerging technique for strengthening structures", Department of Innovation Engineering, University of Lecce, via per Monteroni, 73100 Lecce, Italy, Oct. 2006.
[3] A Kamiharako, T. Shimomura, K. Maruyama, H. Nishida, "Stress transfer and peeling-off behaviour of continuous fiber reinforced sheet-concrete system". *In Proc. 7th East Asia-Pacific Conference on Structural Engineering and Construction*; Tokyo, 1999. pp. 1283–1288.
[4] J.M., Sena Cruz, J.A.O., Barros, R. Gettu, "Bond behavior of near-surface mounted CFRP laminate strips under monotonic and cyclic loading." Rep. DEC/E-04, Department of Civil Engineering, University of Minho, Guimarães, Portugal, 55 pp. 2004.
[5] F. Al-Mahmoud, A. Castel, R.l François, C. Tourneur, "RC beams strengthened with NSM CFRP rods and modeling of peeling-off failure", *Composite Structures*, Vol. 92, pp. 1923-1930, Jul. 2010.
[6] F. Sayed Ahmad, G. Foret, R. Le Roy, "Bond between carbon fibre-reinforced polymer (CFRP) bars and ultra high performance fibre reinforced concrete (UHPFRC): Experimental study", *Construction and Building Materials*, vol. 25, pp. 479-485, Feb. 2011.
[7] RILEM. "Bond test for reinforcement steel. Beam test." TC9-RC, 1982.